INFLUENCE OF PROCESSING PARAMETERS ON THE SUBSTRUCTURE OF ODS ALLOYS

J. Zbiral[1)], G. Jangg[1)], H.J. Ullrich[2)], G. Korb[3)] and H. Oettel[4)]
1) Institut für Chemische Technologie Anorganischer Stoffe
Technische Universität Wien, 1060 Wien, Getreidemarkt 9/161
2) Institut für Werkstoffwissenschaft, TU Dresden
D-8027 Dresden, Mommsenstraße 13
3) Metallwerk PLANSEE GmbH, A-6600 Reutte/Tirol
4) Institut für Metallkunde, TU Bergakademie Freiberg

Dedicated to Prof. Dr. Peter Ettmayer, Institut für Chemische Technologie Anorganischer Stoffe der Technischen Universität Wien, on his 60th birthday.

ABSTRACT

The processing technology of ODS alloys is treated from the viewpoint of substructure parameters like dislocation densities and crystallite sizes of consolidated and worked materials. The connection between parameters of substructure and tensile properties will be discussed. A concise of substructure changes during mechanical alloying, extrusion, working and recrystallization response shows, that an optimum microstructure can be defined. This optimum substructure is described by a function, which connects the crystallite size and the dislocation density of well processed ODS materials. The defined boundary line condition for substructure parameters allows a quality control, which is based upon measurements of substructure data. Because the tensile properties of ODS alloys are a superposition of a series of parameters, the strengthening contributions from the dispersoids, the crystallite sizes and the dislocation densities will be discussed. The influences of processing parameters on the microstructure are described for a number of commercial and model dispersion strengthened alloys.

INTRODUCTION

Oxide dispersion strengthened (ODS) alloys contain a fine dispersion of high temperature stable oxides in a metal matrix. The dispersion of the oxides - usually Y_2O_3 - improves not only the high temperature strength but also the creep properties. According to current understanding (1, 2, 3, 4), good high temperature properties are expected, if the dispersoids are about 10-20 nm in size and their mean distance is approximately 100-250 nm.
The strength of ODS materials is determined by a series of influences (5, 6, 7, 8), which are given by parameters of the substructure (Equation 1). Because of their poor matrix strength, ODS-Al, Cu and noble metals are used in the fine grained condition. The oxide dispersion

keeps the substructure as fine grained as possible and stabilizes the fine grains up to a high application temperature. The grain size is approximately the mean dispersoid particle distance (9, 10, 11). Thus the strength is increased by small grain sizes and high dislocation densities.

$R_{0.2} = R_m + R_\Lambda + R_\rho + R_d$ Equation 1

R_m	Strength of matrix metal
R_Λ	Strengthening by small grain sizes
	$\approx 6Gb/\Lambda$
R_ρ	Strengthening by dislocations
	$\approx 0.6Gb\sqrt{\rho}$
R_d	Strengthening by dispersoids
	$0.8GbM/\lambda$
	$M = \frac{1}{\cos \psi \cos \varphi}$
	$\lambda = ((\pi/f)^{0.5}-2)(2/3)^{0.5}r$
φ	Angle between tensile axis and gliding direction
ψ	Angle between tensile axis and gliding plane
λ	Mean dispersoid particle distance
r	Dispersoid particle size
f	Volume fraction of dispersoids
Λ	Crystallite size
ρ	Dislocation density
G	Shear modulus
b	Burgersvector

Because ODS alloys are solid solution strengthened, there is no need to increase the strength by a fine grained, stabilized microstructure. Moreover, creep rupture strengths of coarse grained materials exceed those of fine grained ones by far. Therefore, ODS alloys are secondarily recrystallized to establish a structure of coarse elongated grains. Consequently, the strength of ODS alloys is controlled only by the strength of the matrix alloy and the contribution of dispersion strengthening.

The formation of long elongated grains is commonly understood to be a secondary recrystallization (sRx). Therefore the primary grain size must remain under a critical maximum grain size to allow sRx (Equation 2):

$$\Lambda = \frac{4r}{3f}$$ Equation 2

TABLE 1: Investigated ODS Alloys and Processing Parameters

Alloy	Milling Time (h)	Extrusion Temperature (K) Extrusion Ratio	Working Temperature (K)
Ni/0.9 Y_2O_3	4, 8, 16, 24	1323-1523/1:20	1323
NiCr20/0.9 Y_2O_3	4, 8, 16, 24	1373-1523/1:10,1:20	973-1473
NiCr20Al6/0.9Y_2O_3	4, 8, 16, 24, 48	1323-1523/1:10,1:20	1273-1473
Cu/0.5-2 Y_2O_3	1, 2, 4, 8, 16, 24	973-1173/1:20	673-973
FeCr20Al6/0.5 Y_2O_3			673-1373
PM 3030	24	1323-1423/1:4-1:20	1273-1373

PM 3030 = NiCr17Al6Mo2W4Ta2/0.9 Y_2O_3 (Trademark of PM-HTM Lechbruck, Germany)

Today ODS alloys are produced by mechanical alloying in high energy ball mills. Dispersoid partition and true alloying during MA are performed by repeated fracturing, rewelding and deformation of metal powder particles by ball-particle-ball collisions. Reflecting the substructure changes, increasing dislocation densities and decreasing grain sizes are observed caused by fracture and deformation of the metal powder particles (12, 13).

The following steps, consolidation and working, are connected with heat treatments, which favor grain coarsening and recovery. Therefore, thermomechanical processing must be considered with respect to the substructure stabilization by the dispersoids, which competes with grain coarsening and recrystallization processes during heat treatments (14, 15). Substructure measurements allow a reliable characterization of the ODS processing technology based upon the determination of dislocation densities and crystallite sizes. Contrary to the technological parameters, extrusion ratio and temperature and degree of working and working temperature, substructure parameters offer relevant information about the condition of the material. The tensile properties will be treated with respect to the contributions from matrix alloy, the dispersion strengthening, the crystallite size and the dislocation densities. The influences of the processing parameters on the substructure parameters during MA, consolidation and working as well as the crucial technological parameters will be discussed.

EXPERIMENTAL

Different ODS alloys were produced by mechanical alloying (MA) of blended powder mixtures of Y_2O_3 with an average particle size of 0.6μm (agglomerates of 20nm primary crystallites) and metal powders. The MA powders were capsuled in mild steel cans, degassed and consolidated by hot extrusion at temperatures between $T_{extr.}$=0.7-0.9$T_{sol.}$. The extrusion ratio varied between 1:4 and 1:24. The investigated alloys as well as the chosen processing

parameters are listed in Table 1.

Parameters of the substructure were characterized by measuring the integral profile line width of X-ray diffraction (XRD) profiles. Evaluation of the profile widths allow calculations of crystallite grain sizes and dislocation densities of milled powders as well as of extruded barsand worked samples. Connections between microstructure and mechanical properties were investigated comparing the substructure parameters and the tensile strength of bulk samples.

X-RAY-DIFFRACTION PROFILE WIDTH ANALYSIS OF ODS ALLOYS

PRINCIPLES OF X-RAY-DIFFRACTION SUBSTRUCTURE MEASUREMENTS. X-ray-diffraction (XRD) patterns offer information about three parameters: lattice structure, texture and substructure. Lattice structure and texture influence the relative intensities of the XRD-profiles and the diffraction angles, which are given by Bragg's Law (Equation 3). The intensities of the XRD-interferences are given by Equation 4. If the ODS material exhibits crystallographic textures, the measured intensities will differ from the theoretical diffraction pattern given by Equation 4.

$$\sin\theta = \lambda\frac{\sqrt{h^2+k^2+l^2}}{2a} \qquad \text{Equation 3}$$

λ	Wavelength of radiation
θ	Diffraction angle
h, k, l	Miller's indices of lattice plain
a	Lattice parameter

$$I \sim |F|^2 H\frac{1+\cos(2\theta)}{2\sin\theta}\frac{1}{V^2} \qquad \text{Equation 4}$$

I	Intensity of XRD-profile
F	Structure Factor
V	Volume of unit cell
H	Frequency of lattice plains

The substructure parameters crystallite size and dislocation density influence the line width of the XRD profiles. The smaller the grain sizes and the higher the dislocation density, the more the line profile will be widened.

There are basically two different groups of parameters, which determine the width of measured XRD profiles. The first ones, the so called apparatus parameters, are influenced by experimental conditions like spectra of used radiation, deviation of the specimen surface from the ideal focussing circle, reflection from the depth of the specimen. The second ones are

caused by deviation of the specimen substructure from the ideal crystal structure. These are small crystallite sizes, which are typical for milled, consolidated and worked ODS products, and high dislocation densities.Supposing now that there are no influences of substructure on the profile line width, a function $g(\varepsilon)$ is defined. Because there are no influences of the substructure, this weight function describes the apparatus and experimental profile line only. Supposing now there are no experimental and apparatus influences on the profile line, a function $f(\varepsilon)$, which describes the physical profile line caused by dislocation densities and crystallite sizes, is defined. As mentioned above, the real profile is a superposition of both; the real profile line width is therefore described by a folding operation of $f(\varepsilon)$ and $g(\varepsilon)$ (Equation 5). Limiting values for the calculation of this parameter integral are given by the condition, that the integrand is different from zero.

$$h(\varepsilon) = \int f(\varepsilon)g(\varepsilon-\xi)d\xi \qquad \text{Equation 5}$$

Dealing with the materials substructure, the unknown is the physical profile function $f(\varepsilon)$. The weight function is usually determined by measurements of XRD profiles of standard samples, which must be essentially free of lattice strains and which must show coarse grains.
If the specimen profile $h(\varepsilon)$ and the weight function $g(\varepsilon)$ are known, there will be two ways to evaluate the physical line profile: The more general one is the evaluation of the Fourier transformations of specimen profile and weight function. These transformations are followed by calculation of the Fourier-coefficients of $f(\varepsilon)$, which allow conclusions about the substructure. The second way, the application of which will be discussed, is the description of the profiles by fitted analytical functions, which are characterized by their profile widths. Discrete evaluation of Equation 5 and the variation of fit parameters give a connection between the line widths (Equation 6), which depends on the chosen analytical functions.

$$\beta/B = f(b/B) \qquad \text{Equation 6}$$

B	Integral profile line width of specimen profile
b	Integral profile line width of standard specimen
β	Physical line width, caused by crystallite sizes and dislocation densities

Grain sizes influence the physical line width according to Scherrer's formula (Equation 7). The influences of lattice strains, which are caused by the dislocations, are given in Equation 8. Assuming that the energy of the lattice strain (Equation 9) is equal to the energy of the dislocations (Equations 10, 11), and that interactions between dislocations are negligible, the dislocation density is proportional to the square number of the lattice strain (Equations 12,

13). The proportionality constant k depends not only on the Burger's vector and the radii of dislocation core and the crystallite, which contains the dislocation, but also on the ratio of edge and screw dislocations.

$$\beta_\Lambda = \frac{C\lambda}{\Lambda \cos\theta} \qquad \text{Equation 7}$$

C Crystallite shape factor (0.9–1.2)

$$\beta_\rho = \eta \tan\theta \qquad \text{Equation 8}$$

η Lattice strain

$$U_\eta = \frac{3\pi}{4}\eta^2 E \qquad \text{Equation 9}$$

$$U_s = \frac{Gb^2}{4\pi}\ln(r/r_o)\rho_s \qquad \text{Equation 10}$$

$$U_e = \frac{Gb^2}{4\pi}(1-\nu)\ln(r/r_o)\rho_e \qquad \text{Equation 11}$$

$$\rho = k\eta^2 \qquad \text{Equation 12}$$

$$k = k(b^2, r, r_o, \nu) \qquad \text{Equation 13}$$

ν Poisson's ratio

r Radius of crystallite, which contains the dislocation or mean half distance between two dislocation lines

r_o Radius of the dislocation core (approximately b)

U Energy, index s refers to screw dislocations, e to edge dislocations, η to the lattice strain

Since there are two unknown parameters, namely the lattice strain and the crystallite size, the characterization of substructure by profile width analysis affords the evaluation of two different specimen profiles at least. Usually this analysis is performed by measurements of all evaluable profiles, calculation of the physical line width followed by a linear regression of $\beta\cos\theta/\lambda$ versus $\sin\theta/\lambda$ (Equation 14).

Anyway the calculation of lattice strains and crystallite sizes affords the correction of the anisotropy of the elastic constants, if profiles of different lattice plains are evaluated. These corrections are done by substitution of the lattice strain by the ratio of the Laue breadth of the stress distribution function and the Young's modulus for the direction perpendicular to the lattice plain of the measured interference (Equation 15).

$$\beta\cos\theta/\lambda = 1/\Lambda + \eta\sin\theta/\lambda \qquad \text{Equation 14}$$

$\eta = \sigma/E_{hkl}$ Equation 15

σ Laue breadth of stress distribution function

E_{hkl} Young's modulus in hkl direction

APPLICATION TO ODS MATERIALS. ODS materials usually exhibit sharp textures, which are caused by consolidation and shaping technologies. Therefore, the number of evaluable interferences is drastically reduced compared with isotropic materials. Based upon the equations mentioned above and upon earlier work (16, 17), a method to characterize even highly textured ODS alloys by means of XRD profile line widths analysis will be discussed. Basis of this method are the measurements of integral profile widths of a (hkl)-lattice interference in the first and second order.

The calculation starts with the correction of the $K_{\alpha 2}$-radiation. Figure 1 gives the ratio of the $K_{\alpha 1}$-line width to the integral profile line width as a function of the ratio of profile eccentricity (Equation 16) to the integral profile line width.

$$e = 2(\theta_{K\alpha 2} - \theta_{K\alpha 1}) \qquad \text{Equation 16}$$

The indices refer to the diffraction angles calculated by Equation 3 using the characteristic XRD radiation wavelengths. Because all the following is done using only the $K_{\alpha 1}$-line width, the index will be dropped.

The connections of specimen line width B, standard line width b and the unknown physical line width β is given in Equation 17, which gives the best correlation between TEM and XRD-data.

$$\beta = B - \frac{b^2}{B} \qquad \text{Equation 17}$$

The next step is a unit conversion from degrees into radians and a separation of the line width caused by crystallite sizes. The crystallite shape factor is assumed to be 1.2

$\beta' = \beta F_1(hkl)$ Equation 18

β' Reduced physical line width

$$F_1(hkl) = \frac{\cos(\theta(hkl))\pi}{180\lambda} \qquad \text{Equation 19}$$

The starting point for separation of lattice strains and crystallite size induced line widths is the

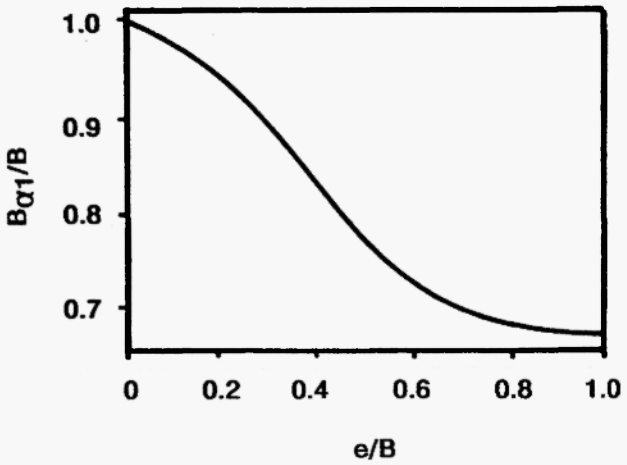

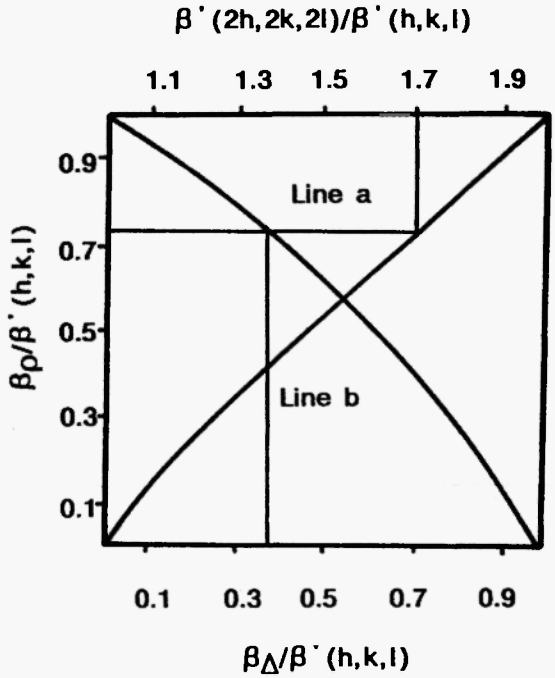

FIGURE 1: Separation of Kα2-Line

FIGURE 2: Separation of Line Widths Caused by Dislocations and Crystallite Size

relation q (Equation 20) of the reduced line widths of the second order interference to the first order interference:

$$q = \frac{\beta' 2h2k2l}{\beta' hkl} \qquad \text{Equation 20}$$

For theoretical reasons the value q must be a value between 1 and 2. A value below 1.3 refers to a polygonized structure, the dislocations are pinned at the dispersoids and thus form the grain boundaries, a value above 1.7 refers to a cold worked, strain hardened material.
Starting now from the ratio q (Figure 2) and following line a, gives the reduced profile width caused by lattice strains, following line b the reduced profile width caused by the crystallite size. Instead of this evaluation, an approximation may be made, which assumes a strictly linear superposition of both and a crystallite shape factor of 1 (Equations 21, 22):

$$\beta_\rho/\beta' = q-1 \qquad \text{Equation 21}$$

$$\beta_\Lambda/\beta' = 2-q \qquad \text{Equation 22}$$

To evaluate the lattice strain, the reduced values must be retransformed (Equation 23).

TABLE 2: Comparison of XRD and TEM Measurements of Crystallite Sizes (μm)

Alloy	Processing	XRD	TEM
ODS-NiCr20	Extruded 1373K	0.18	0.25
ODS-NiCr20	HIP 1273K	0.12	0.22
ODS-NiCr20	HIP 1373K	0.17	0.31
ODS-NiCr20	HIP 1523K	0.45	0.65
ODS-FeCr20Al6	Rolled 973K □12mm	0.50	0.50
ODS-FeCr20Al6	Rolled 973K □18mm	0.17	0.26
ODS-FeCr20Al6	Extruded 1423K	0.2-0.4	0.40
ODS-FeCr20Al6	Forged 1373Kϕ12mm	>1	1.6
ODS-FeCr20Al6	Rolled 1373K□12mm	0.26	0.37

Parameters of substructure are calculated according to Equations 23, 12 and 13. The proportion value k is calculated as described in Equations 9-13.

The upper value (Equation 25) corresponds to screw dislocations, the value below (Equation 26) to edge dislocations only.

Since there are usually both types present, Equations 24 and 25 give limiting values for the dislocation density, the actual value lies between the two. Moreover, the logarithmic ratio $\ln(r/r_0)$ must be estimated. For the purpose of substructure characterization the value r is approximated by the radius of the crystallite, which is half of the evaluated crystallite size. Relevance to this estimation is given by the fact, that dispersion hardened alloys usually do not contain many free dislocations within the crystallite grains. The value r_0 is commonly assumed to be approximately the length of the Burger's vector. In any case, a change of the ratio r/r_0 by one order of magnitude changes the logarithmic ratio of both only by a factor of 2.3. Consideration of the inaccuracies of the other calculation steps shows, that any inaccuracy brought about by these estimations is negligible.

$$\eta = \sin\theta(hkl)/(\lambda\beta_D) \qquad \text{Equation 23}$$

$$\Lambda = 1/\beta_\Lambda \qquad \text{Equation 24}$$

$$k_s = 6(1+\nu)\pi^2/(b^2\ln(r/r_0)) \qquad \text{Equation 25}$$

$$k_e = 6(1-\nu^2)\pi^2/(b^2\ln(r/r_0)) \qquad \text{Equation 26}$$

Results of crystallite size measurements, which were measured by XRD as well as by TEM, are given in Table 2. Because the finer grains influence the profile width of XRD peaks stronger than the larger ones, the crystallite sizes of XRD measurements are below the TEM values. Generally the TEM values are approximately 0.1 μm higher, but there is a satisfactory

correlation between both methods. The great advantages of XRD-characterizations are the short time spent on sample preparation and measurement and the possibility to characterize substructures of large areas (10x10mm) in one run (TEM-area 10x10µm!).

DEVELOPMENT OF SUBSTRUCTURE DURING MA AND EXTRUSION

Changes of microstructure during milling are evoked by repeated fracturing, welding and deformation of metal powder particles due to the ball-particle-ball collisions. The collision events raise the dislocation density from starting values below $10^{10}/cm^2$ to saturation values of approximately $10^{13}/cm^2$ during the first period of milling (Fig. 3). The increase of dislocation densities is followed by a decrease of crystallite sizes.

Substructures of MA powders, which were shortly milled, show grain coarsening, because the insufficient dispersoid partition is not able to stabilize the fine grained MA structure. The longer the milling times were applied, the more is the fine grained substructure of the MA product stabilized. This means that continued milling improves the dispersoid partition.

Analogous changes of microstructure are observed during consolidation of milled ODS-powders by hot extrusion at constant extrusion temperatures and ratios. The longer the milling times applied before extrusion, the finer grained the substructures observed after extrusion. On the other hand, the dislocation density of the extruded bars does not depend on milling time, but remains constant within the accuracy of measurement. Consideration of the influences of milling time on the substructure parameters of ODS alloys shows, that the longer the milling times applied, the finer grained are the ODS materials produced. Within the substructure plot of dislocation density versus crystallite sizes, the improvement of dispersoid partition yields a shift of substructures towards smaller grain sizes. Thermomechanical processing of ODS materials with insufficient dispersoid partition yields a shift of substructure in the direction of higher grain sizes. Thermomechanical processing of well processed samples cause a decrease of dislocation densities and an increase of crystallite sizes. The changes of dislocation densities and crystallite sizes are bound to each other. Evaluation of the XRD-substructures of well processed commercial and model alloys, which were consolidated by extrusion, shows that there is a mutual dependence of substructure parameters (Fig. 4, Equation 27):

$$\Lambda = K \frac{1}{\sqrt{\rho}} \qquad \text{Equation 27}$$

K Proportion value (2.5-3.5 for ODS-fcc-alloys)

The definition "well processed" refers to ODS alloys, which show a homogeneous dispersoid

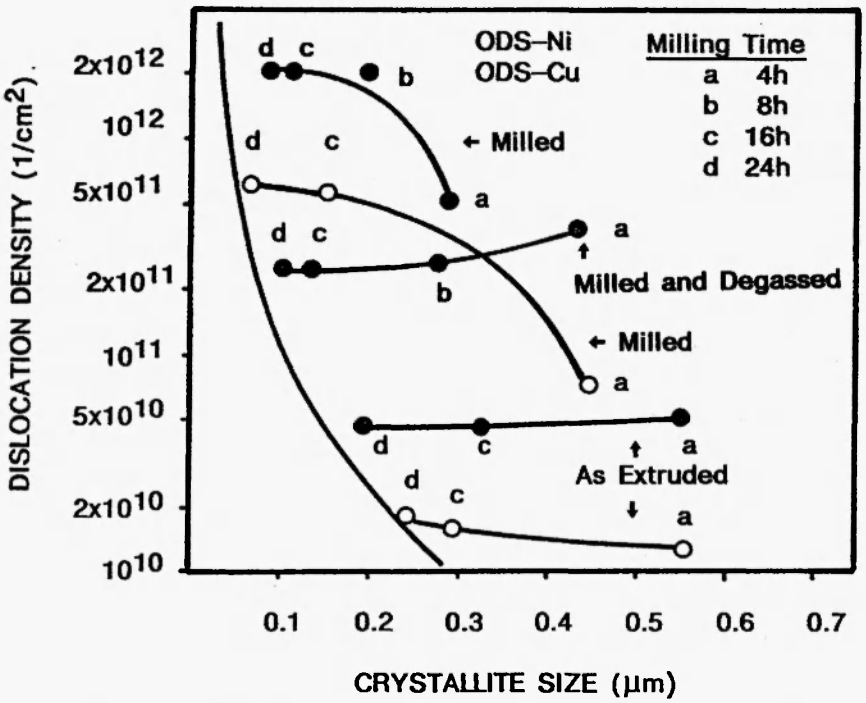

FIGURE 3: Influence of Milling Time on the Substructure of MA Products, Degassed MA Powders and Extruded MA Powders.

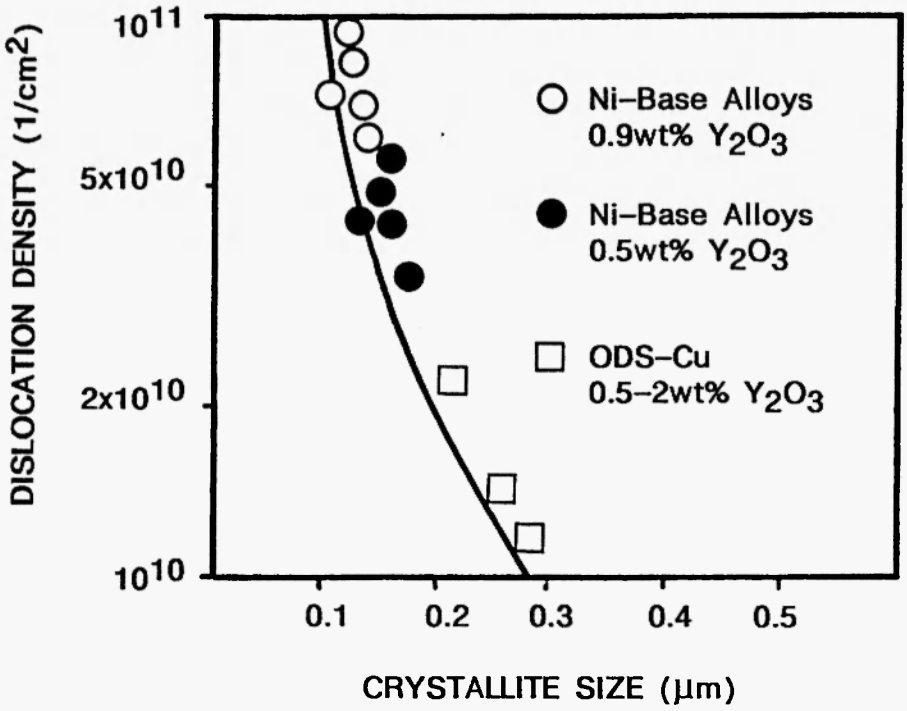

FIGURE 4: Substructures of Well Processed ODS-Bars

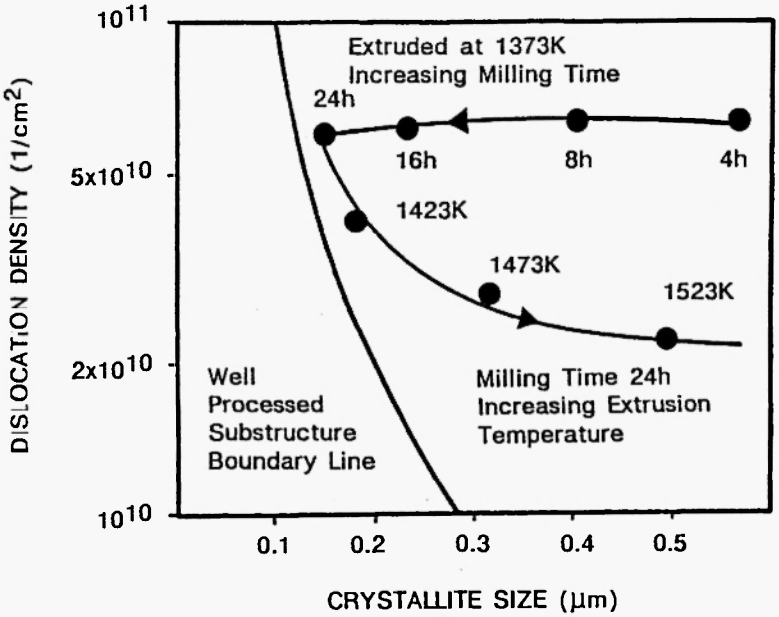

FIGURE 5: Influence of Milling Time and Extrusion Temperature on Dislocation Density and Crystallite Size

partition, which is able to stabilize the fine grained MA structure, e. g. points d in Figure 3. It also refers to ODS materials, that exhibit a coarse elongated structure after sRx. From this point of view, the boundary line condition not only defines the optimum processing history but also the sRx future. The proportion value K varies within the accuracy of XRD-substructure measurements. Equation 27 is supposed to give a boundary line function, which describes the mutual dependence of dislocation density and crystallite size of well processed ODS-products. The evaluation of XRD profile widths allows a fast and reliable determination of boundary line substructures. If the sample shows a boundary line structure, the ratio q of reduced profile widths in Equation 19 varies from 1.28 to 1.35 for fcc-alloys (1.4-1.45 for bcc-alloys). If the actual q-value is higher, the substructure is determined by high dislocation densities. Increasing milling time yields an approach of substructure values to the boundary line, thermomechanical processing yields movements of substructure values parallel and close to the boundary line. If thermomechanical processing causes grain coarsening - this means the ODS alloys are hot overworked -, the values of dislocation densities and crystallite sizes will depart from the boundary line (Fig. 5). Because grain coarsening is a thermally activated process, higher extrusion temperatures result in higher grain sizes. If the extrusion temperature is too high, the values of substructure parameters will depart from the boundary line. The substructure of ODS-NiCr20 extruded above 1373 K shows grain coarsening due to hot overworking. As a result of the grain coarsening by hot overworking, the ODS alloy loses sRx driving force. If the critical grain size is exceeded, the alloy does not recrystallize to form

coarse elongated grains, the sRx-structure consists of fine equiaxed grains, which are formed by normal grain growth. The dislocation densities and crystallite sizes are similar to those of shorter milled samples, which were extruded at lower temperatures. Concerning these two substructure parameters, an ambivalence between milling time and extrusion temperature exists. Therefore the boundary line defined in equation 27 gives a quality control criterion for optimum processing of ODS alloys.

INFLUENCE OF MILLING TIME AND EXTRUSION PARAMETERS ON THE TENSILE PROPERTIES OF EXTRUDED ODS-ALLOYS

Consideration of the changes of microstructure during milling, degassing and extrusion shows that the tensile properties of extruded ODS-bars are determined by the milling time as well (Fig. 6). The longer the milling times applied, the higher the tensile strength values of ODS bars measured due to the improvement of dispersoid partitioning. If the partition is finished, further milling will not increase the strength of the ODS-material after consolidation. This means that constant values of tensile strength of extruded ODS bars will be measured, if the dispersoid partitioning performed by fracturing and deformation of powders during MA is finished.

Comparison of experiments with metal powders of different particle siz, show that the larger the metal powders milled, the longer are the milling times necessary to reach constant strengths (Fig. 6a). While the strength of ODS-Ni-bars becomes constant, when the ODS raw material was milled at least 8 hours, 24 hours milling is necessary to obtain constant tensile strength values for ODS NiCr20 charges. Analogous behaviour is observed for ODS-Cu-bars produced by MA of different Cu powders and following hot extrusion. If the particle size of the Cu starting powder exceeds 125µm, the dispersoids are not partitioned anymore in the Cu-matrix within reasonable milling times and the tensile strength does not reach a constant value. Powder particle sizes influence the minimum milling time especially when fcc-matrix alloys are produced. The finer the starting powders, the lower are the minimum MA-times necessary to achieve a sufficient dispersoid partitioning.

The tensile strength versus elongation plot (Fig. 6b) of differently processed ODS alloys offers more detailed information about the connections between MA and extrusion parameters and tensile properties. The strength of ODS-Ni, which was only blended but not milled before extrusion, is significantly below those of dispersoid free materials. Because these materials do not exhibit a satisfying dispersoid partitioning, the dispersoid particles do not cause strengthening, acting rather as material defects. Even short milling times yield a significant

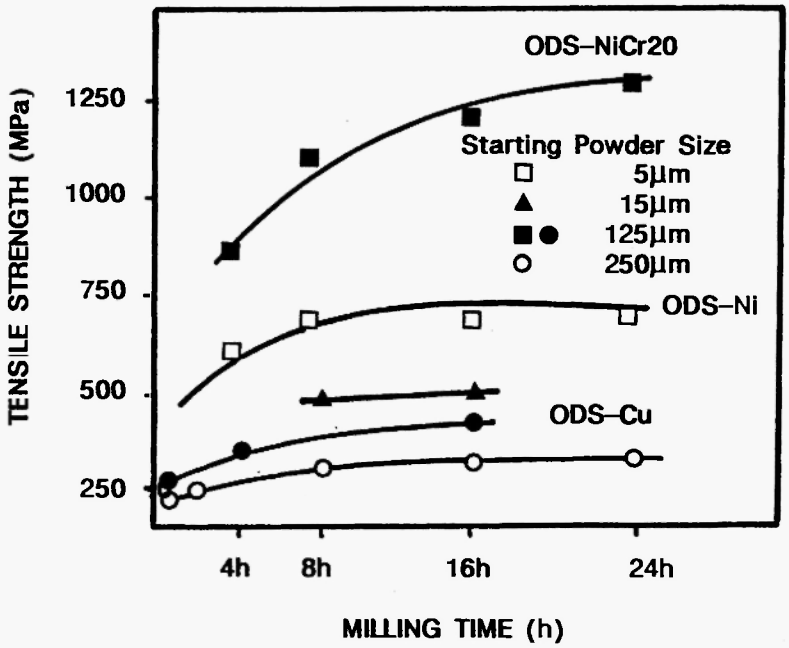

FIGURE 6a: Tensile Strength of Differently Milled as Extruded ODS Alloy

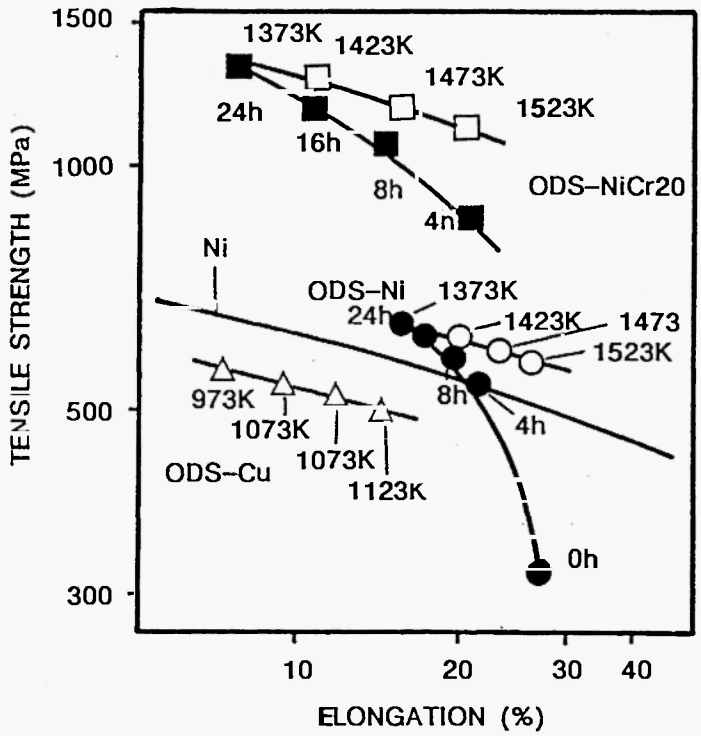

FIGURE 6b: Tensile Strength and Elongation of Differently Processed ODS Alloys

increase of material quality because the tensile strength is increased, while the elongation remains constant. Continued milling causes further increases in strength and decreasing elongations of extruded samples.

On the contrary, rising extrusion temperatures of equally milled and degassed MA products cause a decrease of tensile strength, which is balanced by a significantly increased elongation. The tensile properties of ODS bars, which were extruded at higher temperatures, do not drop down to the values of ODS bars, which were milled shorter but which were extruded at lower temperatures. Because higher extrusion temperatures favor grain coarsening (Fig. 5), the dislocation densities and the crystallite sizes of higher extruded ODS samples are similar to those of shorter milled and lower extruded samples. The strengthening contributions from dislocation densities and grain sizes are, therefore, equal for both materials. The higher strength levels of samples milled longer and extruded at higher temperatures are due to the improved dispersoid partitioning caused by increased milling time. Therefore tensile strength and elongation alter at a higher level.

In analogy to the substructure boundary line, a boundary line exists for tensile properties of ODS materials, which show good dispersoid partition. The mutual dependence of strength and elongation values represents the influence of extrusion parameters on the mechanical properties of ODS alloys. A similar dependence is found for many non-dispersion strengthened alloys; the tensile strength versus elongation couples for pure Ni are plotted in Figure 6b.

WORKING OF ODS-ALLOYS

Considering now the substructure of profile rolled ODS-NiCr20 bars, which depends on the working temperature and the degree of working (Equation 28), we identify three regions of working (Fig. 7):

Region I, which is typical for low working temperatures (ODS-Ni-base <1023K, Fe-base <773K), is characterized by increasing dislocation densities with increasing strain. If a critical value of approximately $10^{13}/cm^2$ is locally exceeded, the material fails by splitting up (alligatoring).

Region III, typical for high working temperatures (ODS-Ni-base >1373K, ODS-Fe-base >1223K), is characterized by dynamic grain coarsening with increasing strain. The grain coarsening is a dynamic effect, because samples, that have only been heat treated show significantly lower grain coarsening rates. The ODS-material not only looses strength; due to the grain coarsening, the sRx driving force is also reduced. The substructure changes caused by region III working, correspond with those of extruded bars, which were hot overworked by too high extrusion temperatures (ODS-NiCr20 extruded above 1423K, Fig. 5).

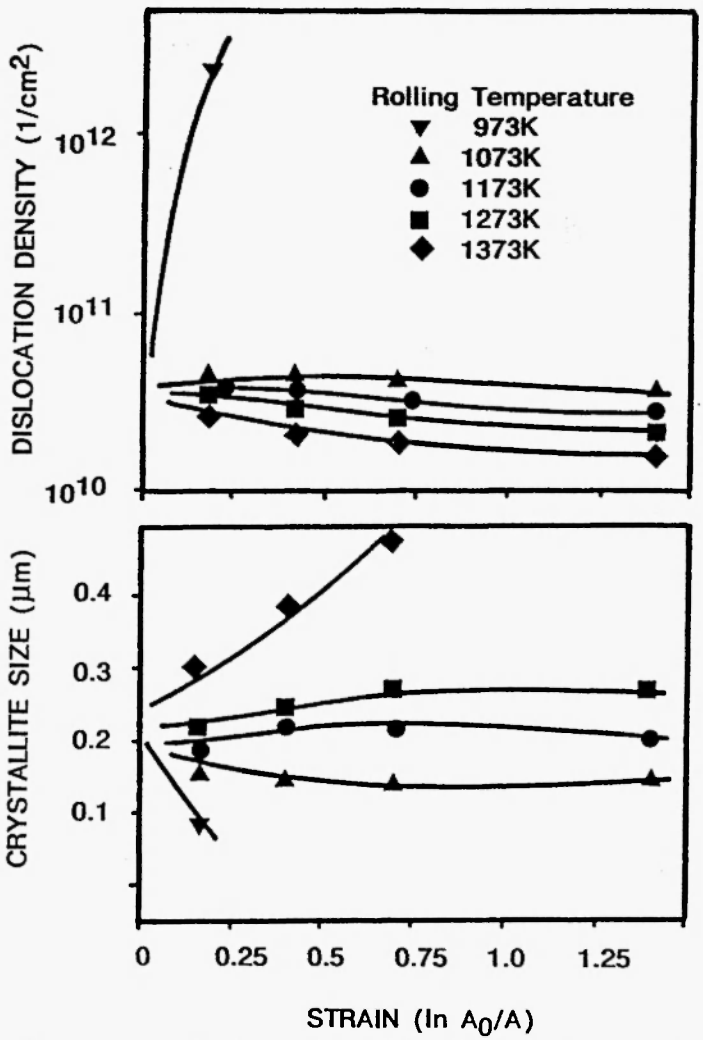

FIGURE 7: ***Influence of Strain and Working Temperature on the Dislocation Density and the Crystallite Size of Profile Rolled ODS-NiCr20***

$\phi = \ln(A_0/A)$ Equation 28

ϕ	Strain
A_0	Area of cross section before working (here: cross section of as extruded bar)
A	Area of cross section after working

In between there is a region II (Fig. 7), where the substructure parameters approach values, which depend only on the temperature of working, but which do not depend on the strain. If the working temperature is increased, the grain sizes are higher and the dislocation densities are lower. Constant working temperature causes constant substructure parameters in the region II working regime. This means, that there is a dynamic equilibrium of creation of

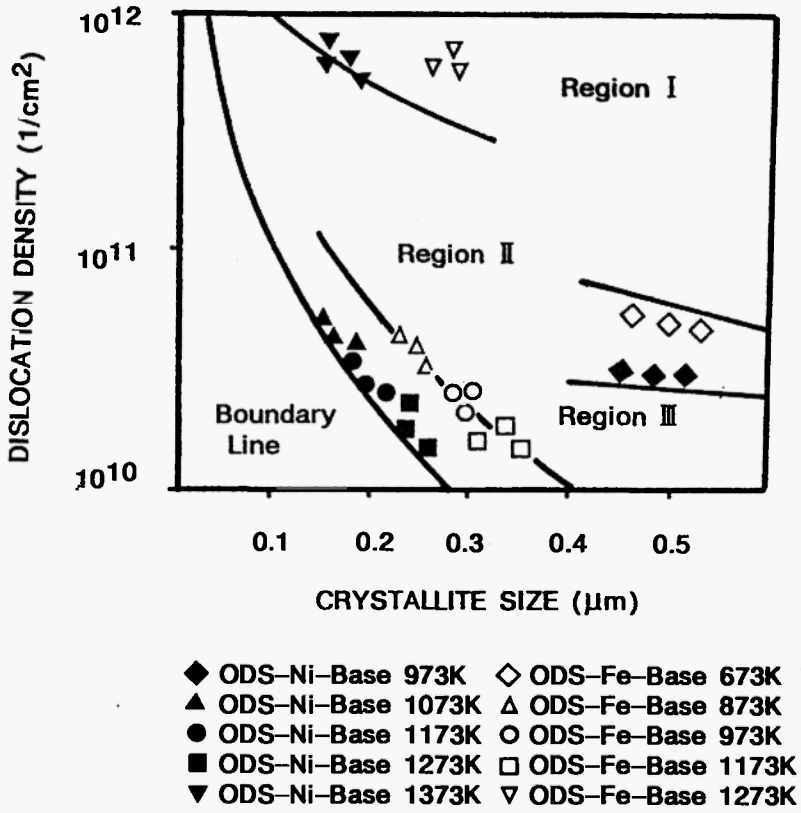

FIGURE 8: Characteristic Values of Dislocation Densities and Crystallite Sizes for the 3 Regions of Working for Fe and Ni-based ODS Alloys

dislocations and recovery as well as grain refinement and grain coarsening. In this regime the dislocation density versus crystallite size plot substructure parameters are close to the boundary line (Fig. 8) defined for well processed ODS-alloys (Fig. 4, Equation 27).

These three regions of working behaviour are typical for many ODS alloys: An analogous substructure parameter diagram may be constructed for profile rolling of ferritic ODS alloys (Fig. 8, 9). Then the regions of working are shifted to higher dislocation densities (the proportion value K in Equation 27 is approx. 6-8, Fig. 8), but the patterns remain basically unchanged. Only the proportion value of the boundary line function describing well processed samples (Equation 27) changes.

Investigation of ODS-Cu, Pt, NiCr20 and γ'-strengthened ODS-Ni-base alloys shows, that the proportion value K for opimum processing conditions varies between 2.5 and 3.5 for all investigated ODS-fcc-matrix metal alloys.

Comparison of ferritic and austenitic ODS-alloys (Fig. 8) shows, that temperature boundaries between the three regions are higher, if Ni-base alloys are worked. This might be due to the higher thermal stability and the lower self-diffusion coefficients of the fcc-matrix. Solid

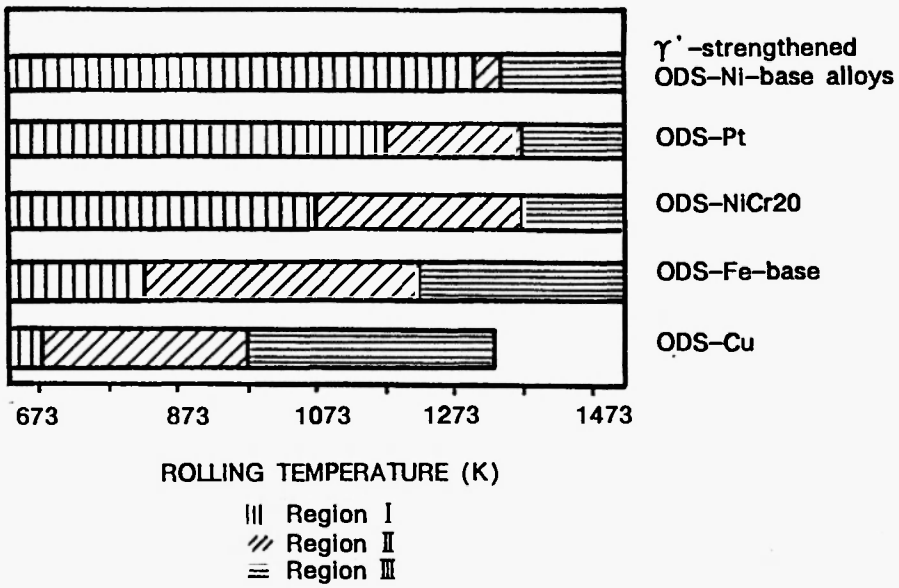

FIGURE 9: Working Regions for Different ODS Alloys

solution strengthening of Ni-base alloys by Al or of Fe-base alloys by Mo and W raises the limiting temperatures as well.

The influence of the dispersoid content on the upper limiting temperature of region III is small. But increasing dispersoid contents as well as γ'-strengthening raise the lower limiting temperatures of region II, thus narrowing the region II temperature interval. Successful profile rolling of alloys like PM 3030 without losing driving force for sRx and without splitting of the material is only possible in a narrow temperature range of 50K (Fig. 9). Additional strengthening of ODS alloys by higher dispersoid contents and high γ'-volume fractions is therefore limited, because the region II interval becomes too narrow to be kept within technological ODS-processing abilities.

RECRYSTALLIZATION

After consolidation and working, ODS alloys are secondarily recrystallized to establish a structure of coarse elongated grains to achieve good high-temperature properties. The time to fracture of coarse grained materials under high temperature, long-term creep conditions is four orders of magnitude higher than that of fine grained ones. Consequently, the sRx-response of these materials is extremely important for high temperature applications. Therefore, the whole processing technology focusses on the sRx-process, which must yield a structure of coarse, highly elongated and interlocked grains.

Because sRx is driven by the energy of the grain boundaries, sRx will only occur if the grain

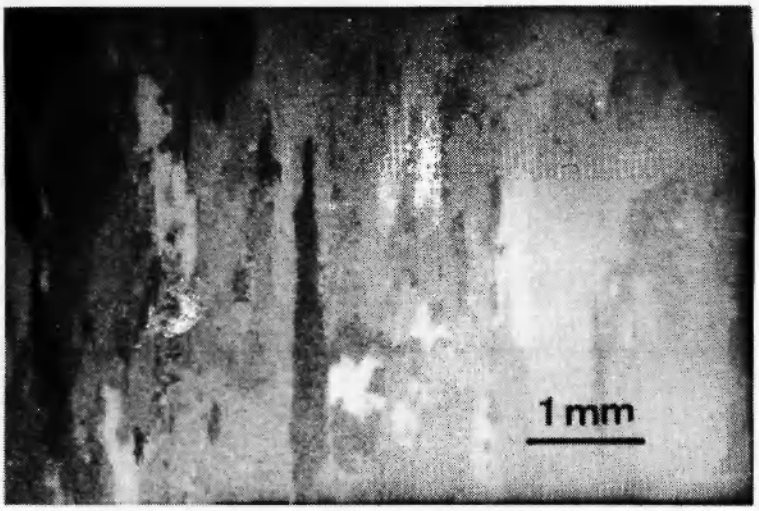

FIGURE 10a: sRx-Response of a Boundary Line Processed ODS-NiCr20 Sheet

FIGURE 10b: sRx-Response of a Boundary Line Processed ODS-NiCr20 Wire (24h milled, extruded below 1373K, region II worked)

size of the as worked material is below the critical one (Equation 2). This condition is necessary but not sufficient for the formation of an elongated coarse grained structure. ODS alloys show a sRx-response with long elongated coarse grains only if the ODS alloys are boundary-line processed during the whole processing technology. This means the ODS alloy exhibits a boundary line substructure (Equnation 27) before the sRx heat treatment.

Boundary line substructures of worked ODS alloys are only achieved if the MA process yields a homogeneous dispersoid partition (Fig. 1&3, 24h milling for ODS-NiCr20, 8h for ODS-Ni). Moreover, the extrusion must not cause grain coarsening (Fig. 5) and the alloy must be worked in the region II temperature range (Fig. 8). Fig. 10 shows the sRx-structure of a boundary-line processed ODS-NiCr20 sheet (Fig. 10a) and of a boundary-line processed profile-rolled ODS-NiCr20 wire (Fig. 10b), which was produced by milling for 24h, to yield a

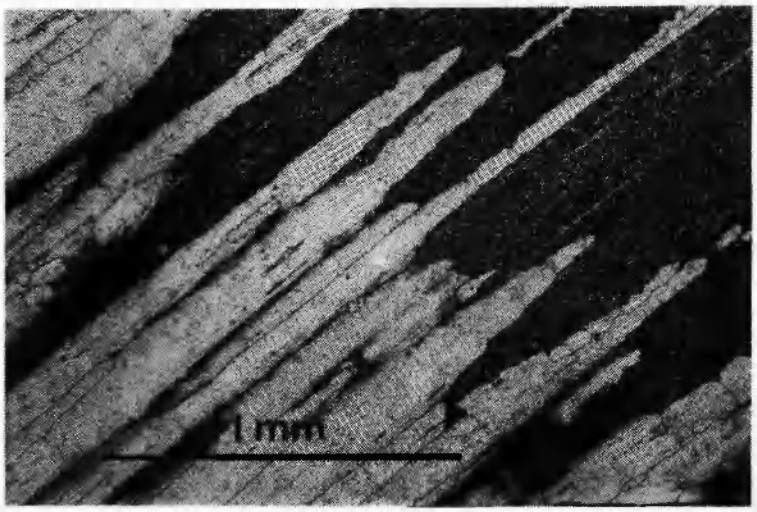

FIGURE 11: sRx-Response of an ODS-NiCr20 Wire, which Was Hot Overworked by Profile Rolling at 1373K (Milling 24h, Extrusion below 1373K)

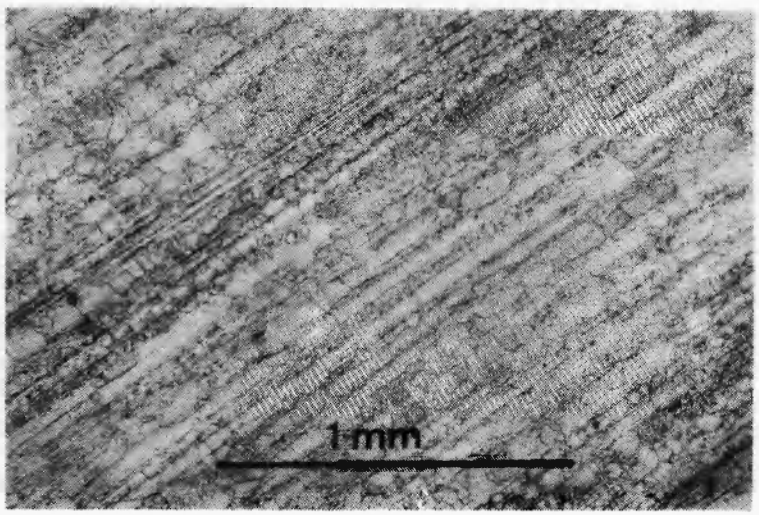

FIGURE 12: sRx-Response of an ODS-NiCr20 Wire, which Exhibits Insufficient Dispersoid Partitioning due to too Short Milling Time (4h milled, extrusion and consolidation analogous to the 24h milled sample)

homogenous dispersoid partitioning. After milling, the MA-powder was consolidated by extrusion below 1373 K, the extruded bar was region Ⅱ worked, to establish a boundary line substructure as shown in Fig. 8.

If the ODS-NiCr20 wires are hot overworked due to region Ⅲ working, they do not recrystallize completely (Fig. 11). Excepted the working temperature, the sample was processed like the ODS-NiCr20 wire shown in Fig. 10b. Hot overworking favors grain coarsening, which drives the substructure away from the boundary line (Fig. 9).

If the dispersoid partition is inhomogeneous, the ODS alloy does not show a boundary line

structure after extrusion and after working. The sRx-structure of an ODS-NiCr20 wire, which was produced from an only 4h milled MA-product, shows fine grains as well as non-elongated coarse grains (Fig. 12). Excepted the milling time, this wire was consolidated and worked at the same processing parameters as the 24h milled product, which showed coarse elongated grains after sRx. If the ODS alloys are cold overworked, there will not only be the danger of splitting during working, but the sRx-structure will consist of small grains with grain aspect ratios (GAR) of approximately 2-4. During cold overworking the dislocation density is increased by one order of magnitude, while the crystallite size is not essentially changed. This increase of dislocation densities drives the substructure parameters away from the boundary line (Fig. 11).

In addition to the crystallite sizes, the dislocation densities influence the sRx-response of as worked ODS alloys. Consideration of the substructure parameters of ODS-alloys, which recrystallize either fine grained or with low GAR, shows that the dislocation densities of these samples clearly exceed the boundary line value for the actual grain size (Equation 27). Then the proportion value K, which is calculated from the measured substructure parameters in Equation 27, is significantly higher than the boundary line value of 2.5-3.5 for ODS-fcc alloys and of 6-8 for ODS-bcc alloys.

If the proportion value K, calculated from the measured substructure parameters, is between 2.5 and 3.5 for ODS-fcc-alloys or between 6-8 for ODS-bcc-alloys (and if the crystallite size is below the critical one, Equation 2), the ODS alloy will recrystallize high with GAR.

From the technological viewpoint the as worked ODS alloys must fulfill both conditions: the crystallite size of the as worked ODS-alloy must remain under the critical one (Equation 2) and the substructure parameters dislocation density and crystallite size must obey the boundary line condition (Equation 27) to guarantee a long elongated coarse grained structure after sRx, which is necessary for long-term, high-temperature applications of ODS alloys.

CONCLUSIONS

The substructure of ODS materials is controlled by milling parameters, extrusion ratio and temperature as well as working parameters during rolling. Milling parameters influence the dispersoid partitioning, which is improved if finer starting metal powders are charged and if the milling time is increased. Extrusion and working temperatures determine grain sizes and dislocation densities.

Optimum processed alloys exhibit a substructure, which obeys a boundary line condition defining a correlation between dislocation densities and crystallite sizes. Sufficient sRx-

response will be observed, if boundary line materials are recrystallized. Consolidated and worked ODS alloys exhibit boundary-line substructures only if mechanical alloying yields a fine homogeneous dispersoid partitioning.

Processing parameters, which cause a departure of the substructure from the boundary line (too high extrusion temperatures, hot or cold overworking), cause non-optimum substructures and, as a result, insufficient sRx-response.

ACKNOWLEDGEMENT

The investigations concerning the connections between substructure parameters and processing parameters were supported by the Austrian Fund for Scientific Research, 1040 Wien, Weyringergasse 35, during the technological project "Substructure and Properties of Materials by Mechanical Alloying" project # 8689 TEC.

REFERENCES

1) E. Arzt: Res Mechanica 31 (1991) 399
2) J. Rosler & E. Arzt: Acta Met. 38 (1990) 671
3) M. Rühle: Z. Metallkde. 71 (1980), 1, 65
4) R.C. Benn in E. Arzt and L. Schultz (eds): New Materials by Mechanical Alloying Techniques, DGM-Verlag, Oberursel 1989
5) M. Slesar et al.: Z. Metallkde. 72 (1981) 423
6) E. Hornbogen in P. Haasen et al.: Strength of Metals and Alloys, ISCMA 5 Pergamon Press 2 (1979), 1337
7) E. Orowan: Discussion Symposium on Internal Stresses, Institute of Metals, London 1948
8) L.M. Brown and R. K. Ham: Strengthening Methods in Crystals, Elsevier, Amsterdam 1971
9) G. Jangg et al.: Radexrundschau (1986) 169
10) G. Jangg et al.: Aluminium 51 (1975) 641
11) H. Oppenheim: Z. Metallkde. 74 (1983) 319
12) J.S. Benjamin in P.H. Shingu: Mechanical Alloying, Metal Sciences Forum 88-90 (1992) 1
13) J. Zbiral et al.: ibid. p. 17
14) J.J. de Barbadillo in P.H. Shingu: Mechanical Alloying, Metal Sciences Forum 88-90 (1992) 167
15) G. Korb & D. Sporer in E. Bachelet et al.: High Temperature Materials for Power Engineering, Kluwer Academic Publishing, Dordrecht 1990
16) M. Wilkens: Phys. Status Solidi 2 (1970) 359
17) V.M. Krivoglaz: Metallofizika 7 (1985) 83